Electrical Power and Energy Systems 117 (2020) 105669

Contents lists available at ScienceDirect

Electrical Power and Energy Systems

journal homepage: www.elsevier.com/locate/ijepes

Resiliency analysis of electric distribution networks: A new approach based on modularity concept

Saeed Mousavizadeh[a,*], Tohid Ghanizadeh Bolandi[b], Mahmoud-Reza Haghifam[a], Mojtaba Moghimi[c], Junwei Lu[c]

[a] Faculty of Electrical and Computer Engineering, Tarbiat Modares University, Tehran, PO Box 14115-111, Iran
[b] Faculty of Electrical and Computer Engineering, Urmia University, Urmia, PO Box 5756151818, Iran
[c] Queensland Micro- and Nano Centre, Griffith University, Brisbane, QLD 4111, Australia

ARTICLE INFO

Keywords:
Resiliency
Modularity
Electric distribution network
Microgrids
Dependency

ABSTRACT

Due to specific characteristics of electric distribution systems and their high vulnerability against natural disasters, providing appropriate methods for resiliency analysis and identifying system weaknesses is of great importance. Increasing penetration of distributed generation (DG) resources and developing microgrid (MG) technology provide modularity to distribution networks. Since the system capability in splitting into multi-independent sub-sections benefits its performance in severe circumstances, the level of modularization can be construed as a measure for resiliency analysis. In this study, a novel framework based on the modularity idea is proposed for quantifying the resiliency level of electric distribution systems. Utilizing graph related theories, a new path-based approach is presented to extract the possible set of formable MGs and their servicing areas. Further, electrical and topological features, switching limitations, and reconfiguration options are also included in the MGs exploration process. Then, by introducing new dependency-based indices and considering various uncertainties, the efficiency of the formed MGs and the impact of disasters on the survivability level of the sections are evaluated. In addition, an efficient approximate approach is developed for implementing the method on large-scale distribution networks. The proposed algorithms have been simulated on several case studies with the results confirming their effectiveness and computability.

1. Introduction

With growing dependence of human societies on energy infrastructures, especially the electric power systems, analyzing the vulnerability of such facilities against potential errors has been of great interest [1,2]. In addition, owing to world climatic changes in recent decades, the severity of natural disasters and their related destructive effects have grown substantially [3,4]. Disruptions in social and economic affairs, due to the harmful consequences of such phenomena, highlighted the importance of investigating the resiliency of electric power systems [5]. The resiliency concept examines the ability of a system to tolerate and endure high impact low probability (HILP) events [6–8]. Natural disasters such as windstorm, floods, droughts, thunderstorm, earthquake or man-made events such as terrorist acts and cyberattack are the catastrophic events with high impact and low probability which can have destructive effects on electric power system [9]. Hence, it is essential to analysis the resiliency of power system against these HILP events to efficiently implement the necessary actions to reduce the effects of them in the operation and planning process of power systems.

In case of severe weather conditions, cooperating with the upstream network to supply the loads may not be conceivable [10,11]. Particular operational constraints of distribution systems, specific structures, extendedness, and diversity of the employed components account for the vulnerability in case of disasters [12,13]. Accordingly, recent research has focused on providing proper approaches for evaluating the resiliency of distribution systems and designing appropriate strategies for responding to long-term planning issues [14–16].

The frameworks proposed for resiliency assessment of electric distribution systems can be categorized into two groups. In the first category, stochastic frameworks and probabilistic approaches are applied to model the event intensity and examine its impacts on the system performance [17–25]. Since estimating the severity of the disasters and diagnosing the fragile components (through calculating their failure probabilities) are the essential tasks, the mentioned approaches are generally applied to analyze the system behavior in upcoming severe

* Corresponding author.
E-mail address: Saeed.mousavizadeh@modares.ac.ir (S. Mousavizadeh).

https://doi.org/10.1016/j.ijepes.2019.105669
Received 4 July 2019; Received in revised form 9 October 2019; Accepted 29 October 2019
Available online 06 November 2019
0142-0615/

weather conditions for short-term horizons. This is because of the fact that investigating the possible damages imposed by such events is more predictable for near future days. Due to the imprecise prediction of severity of such catastrophes in longer horizons (because of their extreme volatile nature), and the lack of adequate information about the equipment fatigue and operation conditions in distribution networks, probabilistic-based approaches may confront serious challenges in resiliency analysis of the expansion plans. In other words, such methods do not provide solid foundations for analyzing the benefits of the investment options from the resiliency viewpoint.

In the second category of studies [26–33], the system resiliency is evaluated utilizing robust optimization-based frameworks and employing defender-attacker models. In these approaches, the operator measures the performance for the worst-case contingencies by considering various attack levels (severity of the event). The mentioned frameworks quantify the resiliency based on the maximum damages inflicted to the system owing to such worst incidents. However, extracting the mentioned worst cases for being employed in expansion studies is again challenging. Moreover, applying the worst-case measures for examining the future reinforcement plans will result in fragile and vulnerable systems against the contingencies with higher intensities. For this reason, such measures do not provide appropriate feedbacks for directing the investment plans and realizing the future resilient systems.

In addition, development of smart grid technologies brings modularity to distribution systems. By utilizing DG resources, load control options, and switching devices, isolated self-provided modules called MGs, can be formed in the network. Independent functioning of these modules allows for robust energy providing and thereby reducing vulnerability in case of severe events. In other words, enhancing MGs formation capability make an outstanding opportunity for improving the resiliency in distribution systems.

Therefore, to quantify the resiliency aspects in electric distribution systems, a comprehensive framework based on the modularity idea is proposed in this paper. In this method, the modularity level of the system is measured by examining its ability in splitting into independent self-provided MGs. Utilizing graph related theories, topological and electrical properties of distribution systems are properly considered in the MGs discovering process. Benefits of applying different items such as reconfiguration and load control capabilities are also investigated [23]. In addition, an efficient approximate technique is introduced to enhance the computability when dealing with large-scale distribution networks.

Moreover, to increase the applicability of the framework in appraising the expansion plans, an efficient technique is proposed to incorporate different uncertainties. In addition, by employing a probabilistic framework, and introducing the idea of parent MGs, impacts of upcoming events are also analyzed. This option enhances the efficiency of the framework when diagnosing vulnerable sections for the short-term horizons. Based on the above, the most important contributions of this paper can be categorized as follows:

- Introducing a novel conceptual framework to assess the resiliency of distribution system based on its modularity level, which is beneficial for being employed in the both short-term and long-term studies.
- Presenting new dependency-based indices for quantifying the resiliency concept and providing appropriate feedbacks to direct the expansion plans wisely.
- Proposing a novel path-based method for exploring the possible set of formable modules, and introducing efficient techniques for extracting the best arrangement of MGs.
- Investigating the impacts of the severe events on the system resiliency, MGs survivability, and vulnerability of the sections; considering various uncertainties, switching capabilities, and load control options.

The other sections of this paper are as follows. In Section 2, the background of the proposed approach for resiliency quantification is discussed. In Section 3, the search process for finding the formable MGs is described. Section 4 examines the efficiency of the proposed algorithm by performing several simulations on two modified 85-bus and 119-bus test systems, and a real distribution network. Finally, conclusions are given in Section 5.

2. Modularity concept

Modularity is a general concept, typically defined as a degree to which elements of a system can be grouped with minimal dependency across groups [34]. In the resilience context, modularity states that the functionality of a system should be distributed through various nodes of the system so that if a single node is damaged or destroyed, the rest of the nodes will continue to function [35]. This concept has been well recognized by the academia and industry, and has recently gained special attention in the field of vulnerability analysis of the critical infrastructures such as water, energy, transportation, information and communication systems [36–38]. In the field of electric power system, the modularity has been utilized in several papers for identifying the critical areas of the power grid [39–41] or sustainable design of the components [42,43].

In [37,38], the vulnerability of the transmission network of the China power grid under terrorist attacks has been analyzed. In those papers, the concept of modularity was employed to address the problem of assessing the quality of the community structures. Each community consists of a group of elements, which are relatively inter-connected, yet sparsely associated with the other groups in the network. Similarly, in [39] a quantitative community-based method has been developed to diagnose the weak points of the Italian power transmission grid emphasizing on the connectivity characteristics of the network.

However, the proposed methods have mainly investigated the vulnerability of the transmission systems from topological aspects. They are not able to incorporate electrical constraints, utilization of the smart grid facilities like distributed generations, MGs, and the special topological features of the distribution networks.

Therefore, in this paper for the first time, the modularity concept is utilized for resiliency analysis of the electric distribution systems. In this paper, the modularity level for a system is defined based on its ability for splitting into independent self-provided sub-systems called modules. In other words, each module is a MG, which is able to provide its loads through its own power supplies. Capacity of the generation units and switching capabilities affect the system decomposability. For example in Fig. 1, thanks to more numbers of the installed sectionalizers at the network *a*, more modules or MGs can be formed compared to the network *b*. After an event, according to the fault location and extent of damages, only one of the mentioned MGs (*MG1*, *MG2*, or *MG3*) in network *a*, can be formed to supply the consumptions.

On the other hand, the efficiency of a module is defined based on its amount of consumptions and the level of dependency on system components. The dependency feature models the reliance of a module on the system equipment for proper operation. Evidently, these two factors have conflicts with each other. Efficient modules provide more loads with a few numbers of elements.

For example, in network *a*, *MG3* provides more loads than the other formable MGs (*MG1* and *MG2*), but because of containing more elements, it suffers from higher dependency. Finally, based on the efficiency of the formable MGs, the system resiliency can be evaluated. This process is described in detail in Section 3.

In addition, being included in the formable MGs influences the vulnerability of the load points. For example, since load *L1* is involved in all of the formable MGs, then supplying this load after the event is more probable than the other loads. Due to insufficient capacity of the connected DG, load *L5* is not served in any of the mentioned MGs. Load *L4* is included only in one MG which can be supplied only when all of

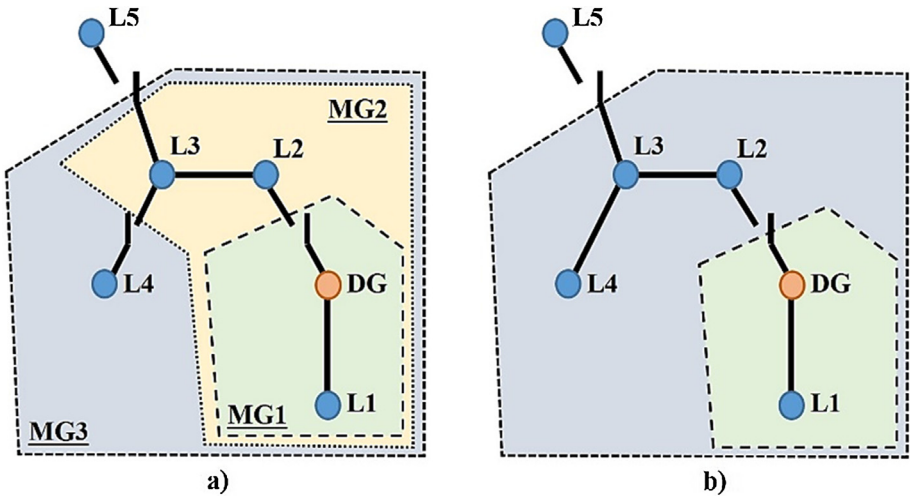

Fig. 1. Impact of the existing switching capability at the network on the modularization.

the required elements for forming *MG3* (the lines, poles, and the other elements) are in the undamaged state. Consequently, *L1* and *L5* have the lowest and highest vulnerability degrees, respectively. In addition, since the status of the *L2* for being included in formable MGs is similar to that of *L3*, thus, their functioning against the event will be the same.

3. Proposed approach

Extracting the set of formable MGs in distribution networks and their efficiency assessment are the main steps of the proposed algorithm. In addition, topological and electrical constraints should also be observed in the search process.

3.1. Exploring the MGs

Initially, based on the location of the switching devices, the network is sectionalized into several sub-systems. The lines with switching capability are considered as the links between the sections. For example, the sample network depicted in Fig. 2 includes six sections and six links.

In addition, in each formable MG, there should be at least one section including a DG unit with voltage and frequency controlling option. These sections are defined as the masters. In Fig. 2, only *S4* is considered as the master. Furthermore, for satisfying the connectivity and radial topology constraints in each MG, there should be at least one path between the sections involved in that MG. For this purpose, a path-based approach is proposed which benefits utilization of the master sections and neighbor analysis in the search process. In the following explanations, symbols S and S_m are utilized to represent the set of the network sections and set of the masters, respectively. In Fig. 2, set S includes sections *S1*, *S2*, *S3*, *S4*, *S5*, and *S6*, while set S_m includes only *S4*.

In this approach, all the existing paths between any of the two non-identical sections from the sets S and S_m will be explored. In path-finding process, a master section is considered as a destination. As a result, for a network with n numbers of the sections and n_m masters, the path-finding process will be performed $n_m \times (n-1)$ times. Breadth-first search (BFS) algorithm [44] is utilized for this purpose.

After finding a path between any of the two members of the S and S_m, the sections included in that path will be considered as a MG that observes topological constraints. This MG is stored in set TMGs. Next, according to the load consumptions and DG capacities of the involved sections, validation of the power balance and load flow constraints will be checked for the explored MG. Hence, In each explored MG with a radial configuration by considering a master DG as a slack bus, the following electrical constraints should be checked by running the backward-forward sweep load flow [45]:

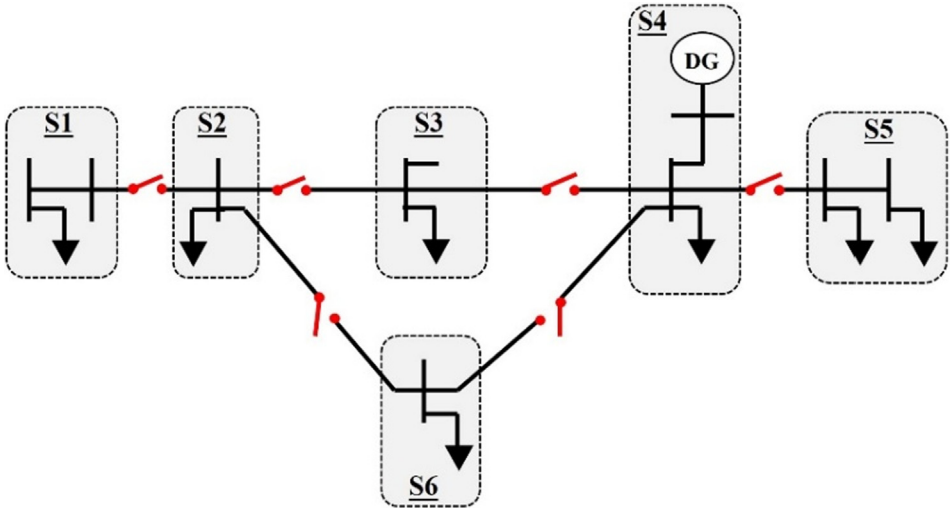

Fig. 2. The sample network.

$$\sum_{m=1}^{N_{DG,k}} P_{m,k}^{DG} - \sum_{i=1}^{N_{Load,k}} P_{i,k}^{Load} = 0 \quad \forall \text{ MG}_k \in TMGs \tag{1}$$

$$- P_{flow,l}^{Max,k} \leqslant P_{flow,l}^{k} \leqslant P_{flow,l}^{Max,k} \quad \forall\, l \in \text{MG}_k \tag{2}$$

$$- Q_{flow,l}^{Max,k} \leqslant Q_{flow,l}^{k} \leqslant Q_{flow,l}^{Max,k} \quad \forall\, l \in \text{MG}_k \tag{3}$$

$$0.9 \leqslant V_{i,k} \leqslant 1.1 \quad \forall\, i \in N_{Bus,MG_k} \tag{4}$$

$$- \delta_{\max} \leqslant \delta_{i,k} \leqslant +\delta_{\max} \quad \forall\, i \in N_{Bus,MG_k} \tag{5}$$

where $P_{m,k}^{DG}$ and $P_{i,k}^{Load}$ denote the generated active power of DG_m in MG k and the supplied active power of the load connected to bus i at MG_k. The Eq. (1) ensures the active power balance at each MG belongs to TMGs. $N_{DG,K}$ and $N_{Load,k}$ are the number of DGs existing in MG_k and the number of load buses in same MG, respectively. Eqs. (2) and (3) represent the limits of the active and reactive power flows of the lines belong to MG_k. $P_{flow,l}^{k}$ and $Q_{flow,l}^{k}$ denote the active and reactive power flows of line l in MG_k. $P_{flow,l}^{Max,k}$ and $Q_{flow,l}^{Max,k}$ are the maximum active and reactive power flow limits of the line l, respectively. $V_{i,k}$, $\delta_{i,k}$ and $\delta_{\max}$ denote the voltage magnitude of the bus i at MG_k, voltage angle of the bus i at MG_k and maximum limit of the voltage angle, respectively. m and i are also the index of the DGs and buses in MG_k, respectively. N_{Bus,MG_k} is the number of buses existing in MG_k. Eqs. (4) and (5) represent the limits of the bus voltage magnitude and angles, respectively. It is important to notice that if the DG m is selected as a slack master unit, the voltage magnitude of the corresponding bus is set at the controlled value and the voltage angle of the mentioned bus is set to zero.

If these electrical constraints are also valid, this MG is added to the set EMGs whereby neighbor analysis phase will be performed; otherwise, the process is repeated by examining another path. This discovered MG is also called the host MG for the sections included in the path. In the neighboring stage, by applying the network adjacency matrix, all the neighbor sections of the discovered MG are explored. This set of neighbors is called Neigh. If the adjacency matrix of the network calls A, a_{ij} is the element of matrix A in row i and column j. This matrix is represented as follow:

$$A = [a_{ij}] \tag{6}$$

$$\text{Where: } a_{ij} = \begin{cases} 1 & \text{if section "}i\text{" is connected to section "}j\text{"} \\ 0 & \text{otherwise} \end{cases} \tag{7}$$

Using the adjacency matrix presented in (6), if the condition presented by (8) is satisfied, then (9) represents the neighbor sections set of the MG_k as follows:

$$\text{If} \quad a_{ij} = 1 \quad \forall\, i \in MG_k \;\; \& \;\; \forall\, j \notin MG_k \tag{8}$$

$$\text{Then:Neighs } (\text{MG}_k) = \{S_j\} \tag{9}$$

where S_j denote the set of the explored neighbor sections. For example, in Fig. 2, by extracting the adjacency matrix of the depicted network, for a MG, which includes the sections *S3*, *S6*, and *S4*, the amount of a_{45}, a_{32} and a_{62} would be equal to one, which indicate that the set {*S2*, *S5*} are the Neigh set of this MG.

Then, by merging the involved sections of the extracted MG with all combinations of its Neigh members, new MGs, which satisfy topological conditions, are generated. In other words, the neighboring process ensures the connectivity constraint in the newly formed MGs. For example, in Fig. 2, by merging MG: {*S3*, *S6*, *S4*} and its Neigh set {*S2*, *S5*}, three MGs can be formed as follows: {*S3*, *S6*, *S4*, *S2*}, {*S3*, *S6*, *S4*, *S5*}, and {*S3*, *S6*, *S4*, *S2*, *S5*}. Further, to guarantee the radial configuration for the discovered MGs, minimum spanning tree (MST) structure [46] is selected for them. Then, these new MGs are examined sequentially and in case of redundancy with the MGs which already have been stored in TMGs set, the duplicate MGs will be disregarded, whereby the next combination is investigated; otherwise, the new MG will be added to the set TMGs, and the electrical constraints for that are checked. For performing the power flow calculations using backward-forward load flow, MST structure is utilized.

The radiality constraint in a distribution network is identical to the spanning tree constraint in graph theory [47]. In other word, in order to satisfy the radiality constraint, a MST structure should be extracted for each discovered MGs. The MST in an undirected graph with the weighted edges, is a tree subgraph of that graph and the sum of its weights is the minimum possible. This problem is well-addressed in [47]. Typically, the MST problem for a distribution network represented by a planar graph G with n vertices, m edges and f faces can be formulated as follows:

$$\text{Minimize:} \sum_{i,j} \omega_{ij} b_{ij} \tag{10}$$

Subject to:

$$\sum_{j \in N_i} b_{ij} = 1 \qquad 1 \leqslant i \leqslant n-1 \tag{11}$$

$$\sum_{l \in M_k} \sum_{p \in S_{k,l}} d_{(k,l),p} = 1 \qquad 1 \leqslant k \leqslant f-1 \tag{12}$$

$$\text{For all m edges in G:} b_{ij} + d_{kl,e} = 1 \tag{13}$$

where, b_{ij}, ω_{ij} and N_i denote the binary variable indicating connection status of the edge between two vertex i and j, weight of the edge connecting vertex i to vertex j and set of the vertices directly connected to vertex i, respectively. In the dual graph of G named G*, $d_{(k,l),p}$, M_k and $S_{k,l}$, refer to the binary variable indicating connection status of the edge (s) between two vertex k and l, set of vertices directly connected to vertex k and set of multiple edges between vertices k and l. Index p indicates the number of the connected edges between two vertex k and l.

The set of the presented constraints in (11), (12) and (13) ensure the spanning tree constraint.

For the depicted sample network in Fig. 2, the extraction process of MST is presented in Fig. 3. Firstly, an undirected graph of the network whose edges is appropriately weighted is created. Then, by selecting the edge with the minimum weight, the next edges are added in ascending order to create a spanning tree with N-1 edges. In Fig. 3(b), the roman numerals represent the order to select the edges in the extraction process of MST. The weights of the graph edges are also indicated above them in Fig. 3(a).

If during the neighbor analysis step, a new MG is added to the set EMGs, before investigating the next paths, the neighboring step will be performed again for that new extracted MG. After examining the neighbors for all of the newly discovered MGs, which are added to set EMGs, the search process is repeated by exploring the next path. Finally, after analyzing the paths, self-provided master sections are also added to the both sets of TMGs and EMGs. Flowchart of the proposed

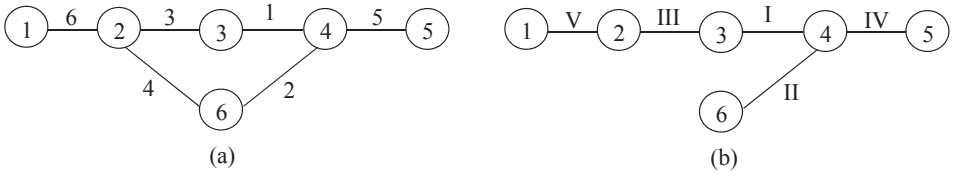

Fig. 3. (a) An undirected graph with weighted edges; and (b) the extraction process of MST.

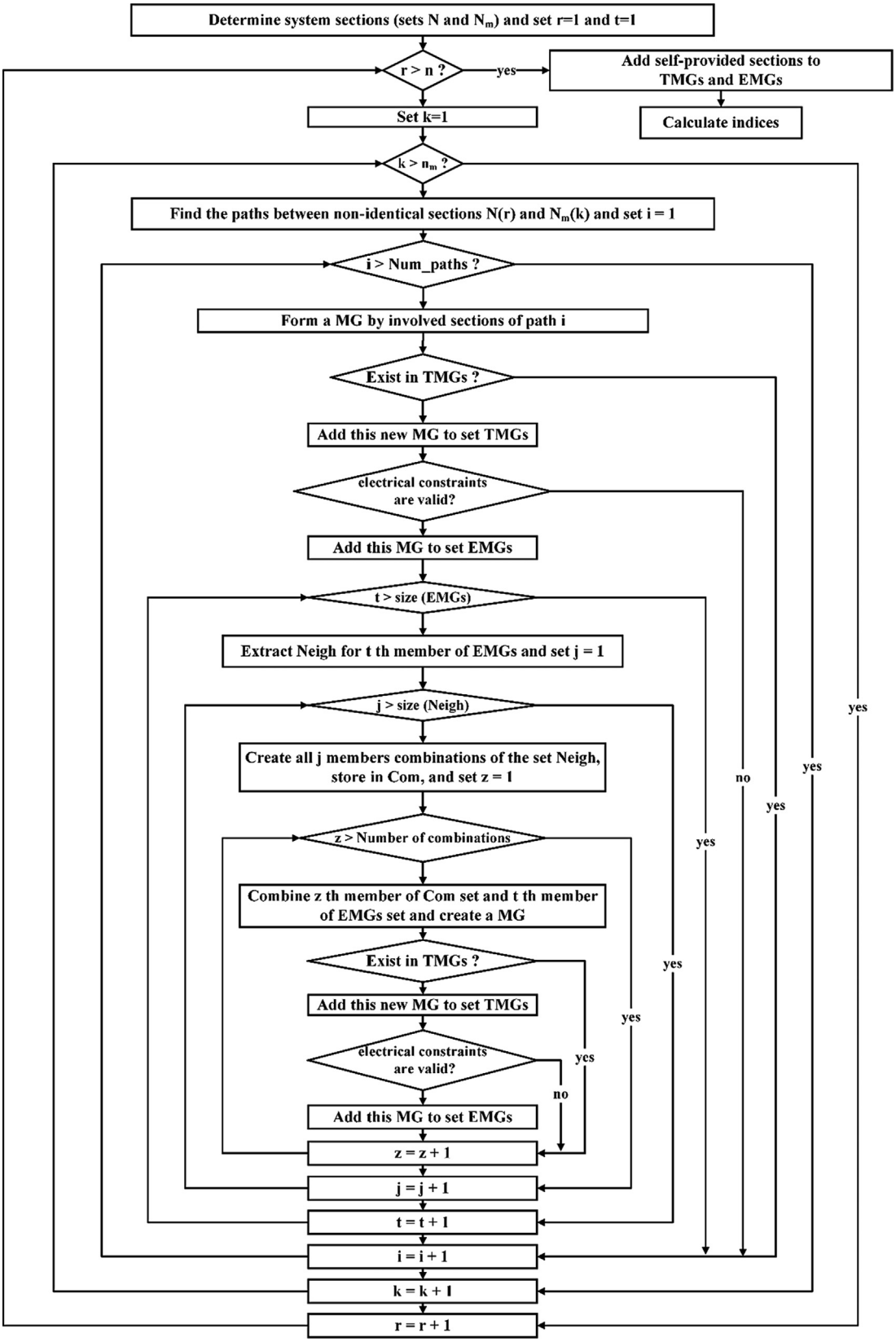

Fig. 4. Flowchart of the proposed algorithm for exploring MGs.

algorithm is displayed in Fig. 4.

In summary, the search process employs two stages for exploring the MGs. Path-finding stage examines the opportunity of forming MGs with the sections included in the path that is explored between any two members of the set S and the set S_m. In addition, performing neighbor analysis phase for each section examines the possibility of forming MGs with the neighbors that are not included in the explored paths. Applying the both path-finding process and neighboring phase for each

section guarantees that the proposed approach will not miss any potential MG, which contains that section and at least one of the masters.

3.2. Efficiency assessment

As mentioned earlier, for measuring the efficiency of a MG, two characteristics should be quantified first: dependency and profitability levels. To calculate the dependency for a discovered MG, it is required to evaluate what portion of the components are used by the MG for providing its connected loads. Because of utilizing the radial structure in distribution systems, we can postulate that the number of the elements required for supplying the consumptions in a MG is consistent with the number of the load points involved in that MG. Therefore, to calculate the dependency level for a MG (MGD index) Eq. (14) is utilized.

$$\mathrm{MGD}_k = \frac{\sum_{s\in k} NoL_s}{\sum_{s\in S} NoL_s} \quad \forall\, k \in \mathrm{EMGs} \tag{14}$$

In Eq. (14), NoL_s represents the number of the load points included in section s. This formulation divides the number of the load points involved in each MG by the total number of the load points in the network. A MG that includes a fewer number of the loads enjoys a higher independency level. In addition, the profitability for a MG represents the amount of consumptions that can be supplied under emergency conditions by that MG. Accordingly, the profitability index (MGPr) for a MG can be defined as Eq. (15). MGs with high MGPr levels provide a large portion of the consumptions.

$$\mathrm{MGPr}_k = \frac{\sum_{s\in k} CoL_s}{\sum_{s\in S} CoL_s} \quad \forall\, k \in \mathrm{EMGs} \tag{15}$$

In this equation, CoL_s represents the amount of the consumptions of the section s. Moreover, efficient MGs include more consumptions with a fewer numbers of elements. Based on this, the efficiency index (MGE) for each MG can be quantified by multiplying its independency and profitability values, as formulated in Eq. (16).

$$\begin{aligned}\mathrm{MGE}_k &= (1-\mathrm{MGD}_k)(\mathrm{MGPr}_k)\\ &= \left(1-\frac{\sum_{s\in k} NoL_s}{\sum_{s\in S} NoL_s}\right)\times\left(\frac{\sum_{s\in k} CoL_s}{\sum_{s\in S} CoL_s}\right) \quad \forall\, k \in \mathrm{EMGs}\end{aligned} \tag{16}$$

Furthermore, if a section is included in the host MGs with lower dependency, then this section will probably experience a more convenient situation in case of sever contingencies compared to the other sections included in highly dependent MGs. Therefore, to differentiate the sections according to this notion, an average dependency level of the host MGs for each section ($\mathrm{AHSeD_s}$) is formulated as Eq. (17).

$$\mathrm{AHSeD_s} = \frac{\sum_{k\in \mathrm{HMGs_s}} \mathrm{MGD}_k}{NumHMGs_s} \quad \forall\, s \in \bar{\mathrm{S}} \tag{17}$$

In this equation, $\bar{\mathrm{S}}$ is the set of sections involved, at least, in one of the discovered MGs, $\mathrm{HMGs_s}$ represents the set of MGs that include section s, and $NumHMGs_s$ denotes the number of the host MGs for the section s.

3.3. System resiliency assessment

The system resiliency can be evaluated based on the efficiency of the host MGs. For this purpose, it is required to examine all possible combinations of the discovered MGs (members of the set EMGs) which do not share a common section. Each arrangement includes a group of MGs, which simultaneously can be formed after the disaster to restore the loads cooperatively.

Utilizing Eq. (18), the value of each arrangement is measured as the sum of the efficiency of the MGs involved in that combination. Furthermore, according to Eq. (19), the system resiliency (SysRes) is the maximum of the calculated values.

$$\mathrm{ArngE}_a = \sum_{k\in \mathrm{InvMGs}_a} \mathrm{MGE}_k \quad \forall\, a \in \Psi \tag{18}$$

$$\mathrm{SysRes} = \max\{\mathrm{ArngE}_a \mid \forall\, a \in \Psi\} \tag{19}$$

In these equations, ArngE_a is the efficiency of the arrangement a, and InvMGs_a represents the MGs involved in that arrangement. The symbol Ψ shows the set of the discovered arrangements.

Then, to find these arrangements, an efficient dynamic programming (DP)-based approach is employed here [48]. In this method, the members of the set EMGs (host MGs) are taken as the possible states. To form the state transition matrix, in each step, according to the previous MGs included in the chosen course and their intersections with the others, the possible states for the next step are extracted. More precisely, each course includes only independent MGs. For example, suppose the set EMGs for a hypothetical network includes four MGs, where *MG1* and *MG2* are the independent ones, but *MG3* and *MG4* share a common section together. Fig. 5 represents the state transition network for the mentioned set. At the first step, all the members of the set EMGs can be selected as an initial state.

In this network, if *MG1* is chosen as the first state, then *MG2*, *MG3*, and *MG4* will be the next possible states. Additionally, at *Step2*, if *MG3* is chosen, due to its intersection with *MG4*, only *MG2* could be taken as the next possible state for moving from *MG3*. Then, by calculating the efficiency of the obtained arrangements, the system resiliency is evaluated.

However, DP algorithms are known to suffer from the curse of dimensionality as the problem size increases. In order to alleviate this issue and accelerate the overall process, we apply an efficient approach, which utilizes decomposition and abandoning techniques to reduce the search space. Dividing the state transition matrix into smaller parts,

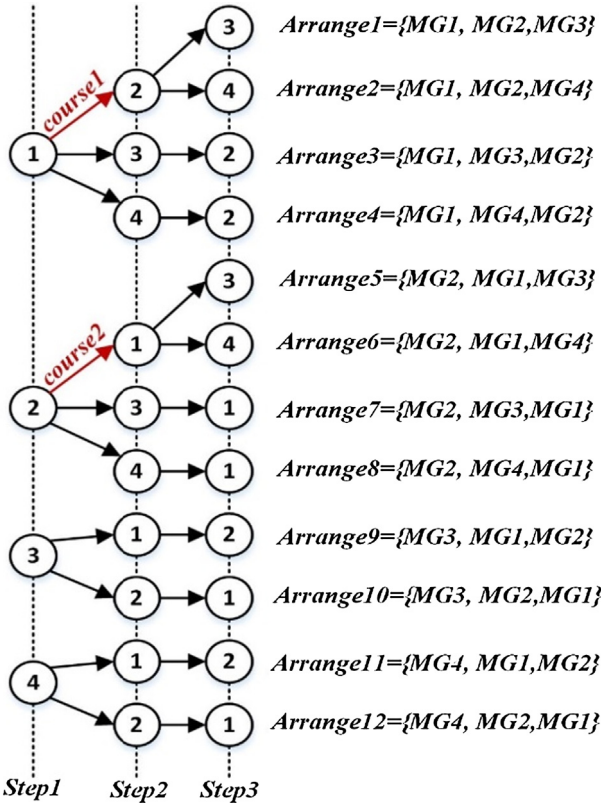

Fig. 5. The state transition network for the considered set EMGs.

based on the independency situation of the host MGs, is the main idea of the decomposition process. For this purpose, first, the host MGs are categorized into several independent groups. Hence, in first step, the following independent groups should be created:

$$G = \{g_1, g_2, ...,g_i\} \qquad \forall\, i \in \Gamma \tag{20}$$

$$g_i = \{MG_{i,1}, MG_{i,2}, ...,MG_{i,n}\} \tag{21}$$

where G is the set of independent groups and g_i is the i'th independent group which includes MGs intersect together directly or indirectly and are completely independent of the MGs included in other groups. n is the number of intersecting host MG in g_i. For example, if MG_x and MG_y, and similarly MG_y and MG_z share a common section; then MG_x, MG_y, and MG_z are included in one group. At the next step, the DP algorithm is utilized for searching the optimal combinations of the MGs in each group. Since the optimal arrangement for each group is entirely independent of the arrangements obtained from the other groups, their union yields the optimal arrangement for the network. Therefore, to calculate the resiliency, we can rewrite Eq. (19) as (22).

$$\text{SysRes} = \sum_{i\in\Gamma} \max\{\ \text{ArngE}_a \ \mid \forall\ a \in \Psi_i\} \tag{22}$$

In Eq. (22), Γ represents the set of the independent groups attained by applying the decomposition technique, and Ψ_i is the set of the arrangements obtained for group g_i.

For example, the host MGs of the previously considered set can be categorized into three groups. As shown in Fig. 6, these groups respectively include {*MG1*}, {*MG2*}, and {*MG3*, *MG4*}. Based on the above, the best combination in each group will be explored by performing DP algorithm in smaller state transition networks compared to the previous case (Fig. 5). Since the first and second groups include only one member, then running the DP algorithm for them only needs one-step simulation. In addition, due to the intersection of the MG3 and MG4, just one of them can be included in the arrangement of the third group. Accordingly, the best arrangement for the network is achieved just by comparing the efficiency of only two combinations {*MG1*, *MG2*, *MG3*}, and {*MG1*, *MG2*, *MG4*} (union of the groups arrangements).

Furthermore, for avoiding unnecessary duplicate calculations, at each step, the MGs included in each course of the DP algorithm are compared with the previously analyzed states until that step in the other courses. In the case of the duplicity of MGs, the course is no longer continued from that step. It is because of the fact that following the mentioned course will not add a new arrangement. For example, in Fig. 5, since the MGs included in *course2* at *Step2* (*MG1* and *MG2*), are the same with the MGs involved in *course1* at *Step2*, therefore, further continuing the *course2* will be abandoned. Base on the above,

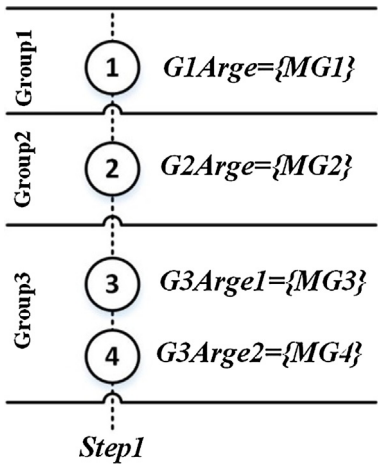

Fig. 6. Implementing the decomposition technique on a hypothetical state transition network.

decomposition and abandoning techniques reduce the simulation burdens and accelerate the calculation process.

3.3.1. Approximate method

Although the proposed method employs a numerical approach for the path-finding process and exploring the MGs, because of the lower generation capacity at electric distribution networks compared to the consumption levels, limited numbers of the switching devices, simple structure, and sparse connectivity of the network, the method is applicable for these types of systems.

However, in large-scale distribution networks, due to the large number of sectionalizers, tie lines, master DGs, and more generation capacities, the search process may encounter high computation burdens. For increasing the applicability of the approach, an approximate technique is presented here. In this method, it is assumed that in each formable MG there should be only one DG unit with the voltage and frequency controlling options. In other words, each MG should include only one master section.

By considering this assumption, the number of the MGs involved in the best arrangement will be equal to the number of the master sections, which is the maximum number of the formable MGs in an arrangement. This issue increases the independency feature of the formed MGs. In addition, utilizing the proposed DP algorithm, for each master section, the most efficient MG that does not contain the other masters will be explored. Forming the MGs with low dependency feature and providing maximum loads through them guarantee getting as near as possible to the optimum solution. However, compared to the main method, the approximate approach does not consider the participation of the masters in forming a common MG.

To implement this approximate approach, path-finding and neighbor analyzing stages are modified. For this purpose, after searching the paths between any of the two members of the sets S and S_m, only the paths that include one master section are maintained for the next investigations and the others will be discarded. In addition, after exploring the neighbors for a MG, the master sections will be eliminated from the neighbor set. This process prevents forming the MGs with more than one master.

3.3.2. Incorporating the uncertainties

To investigate the impact of demand and renewable energy source (RES) uncertainties on the system resiliency, first, considering probability distribution functions (PDFs) and employing scenario generation methods, possible scenarios for the load consumptions and RES generations are extracted. After that, a base EMGs set (EMGs_Base) is formed where the loads and RESs are in their lowest consumption and highest production levels, respectively. Then, considering demand and generation levels at each scenario, the MGs that do not satisfy electrical constraints (energy balance and power flow limits) are removed from the set EMGs_Base, and a new set, called EMGs_*w*, is created correspondingly. Therefore, for extracting formable MGs in each scenario, repeating the path-finding process, and analyzing the topological constraints are not required anymore; consequently, computability is increased. Finally, considering the scenario probability ($\pi(\omega)$), the expected value of the system resiliency (ExSysRes) is calculated as Eq. (23).

$$\text{ExSysRes} = \sum_{\omega\in\Omega} \pi(\omega)\times \text{SysRes}_\omega \tag{23}$$

3.4. Sections survivability assessment

For evaluating the vulnerability of the sections, it is necessary to examine the impact of the events on the system components. For this purpose, special curves have been developed in recent research to calculate the failure probabilities of the equipment in case of disasters such as extreme weather events, earthquake, etc. [49,50,51]. By

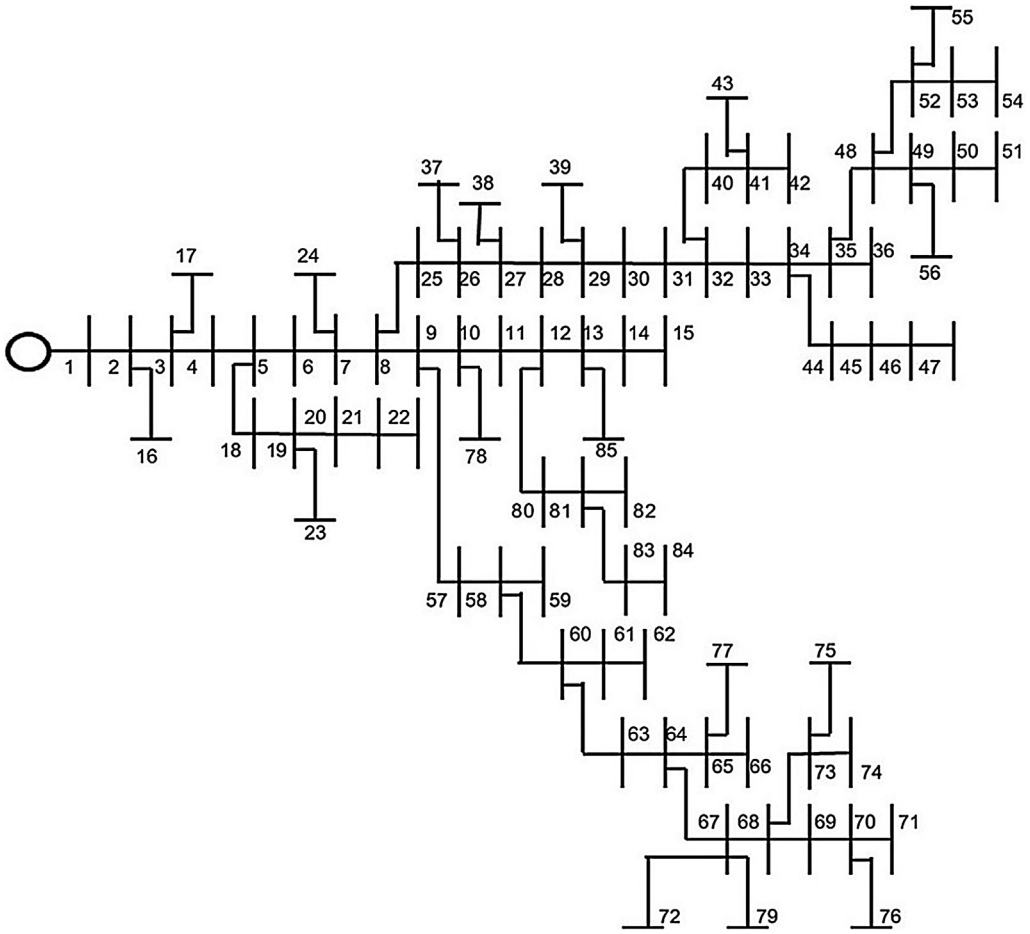

Fig. 7. Test network I.

Table 1
Considered DG installation plans for resiliency enhancement.

Plan1	*Plan2*	*Plan3*	*Plan4*	
500 kW at bus 14	500 kW at bus 30	500 kW at bus 8	190 kW at bus 8	80 kW at bus 30
500 kW at bus 60	500 kW at bus 57	380 kW at bus 9	80 kW a t bus 14	120 kW at bus 34
		120 kW at bus 34	280 kW at bus 19	60 kW at bus 57
			190 kW at bus 60	

employing mentioned fragility curves, availability index for a section ($SeAv_s$) can be formulated as Eq. (24). Then, utilizing the probabilities calculated for the sections, interface links, and generation units included in a MG, the survivability index ($MGSur_k$) can be calculated by Eq. (25).

$$SeAv_s = \prod_{e \in E_s} (1 - f_e) \quad \forall\, s \in \mathrm{S} \tag{24}$$

$$MGSur_k = \prod_{s \in k} (SeAv_s) \times \prod_{\ell \in L_k} (1 - f_\ell) \times \prod_{g \in G_k} (1 - f_g) \quad \forall\, k \in \mathrm{EMGs} \tag{25}$$

In these equations, E_s is the set of the elements (the lines and buses) included in section s, L_k shows the set of the interface links between the sections involved in MG k, and G_k denotes the set of the units required for supplying the MG k. Symbols f_e, f_ℓ, and f_g represent the failure probabilities of the element e, interface link ℓ, and generation unit g, respectively.

In addition, to supply a section, at least one of its host MGs should survive after the event. Based on this, the survivability index for each section ($SeSur_s$) can be defined as the union of the survivability of its host MGs (Eq. (26)). This measure can be applied to diagnose system weaknesses and recognize vulnerable sections in case of the event.

$$SeSur_s = \bigcup_{k \in HMGs_s} (MGSur_k) \quad \forall\, s \in \mathrm{S} \tag{26}$$

Further, if in the set of the host MGs for a section, a MG is a subset of the others, we can use the truncated form of this set for accelerating the computations, without applying any approximation. For more explanations, if MG_m is a subset of MG_n, it means that MG_m can supply the sections existing in MG_n and all the elements of MG_m also included in MG_n. In other word, the supply of the sections of MG_n is dependent to MG_m. Hence, if the MG_n survives the event, definitely MG_m will also survive. The MG_m is called the parent of MG_n. For this reason, we can ignore MG_n in the calculation process of Eq. (26). Based on the above, utilizing this new set, Eq. (26) can be rewritten as (27).

$$SeSur_s = \bigcup_{k \in ParHMGs_s} (MGSur_k) \quad \forall\, s \in \mathrm{S} \tag{27}$$

In this equation, $ParHMGs_s$ is the set of the parent host MGs of the section s. The intersections of the parent MGs should also be considered in the calculation process.

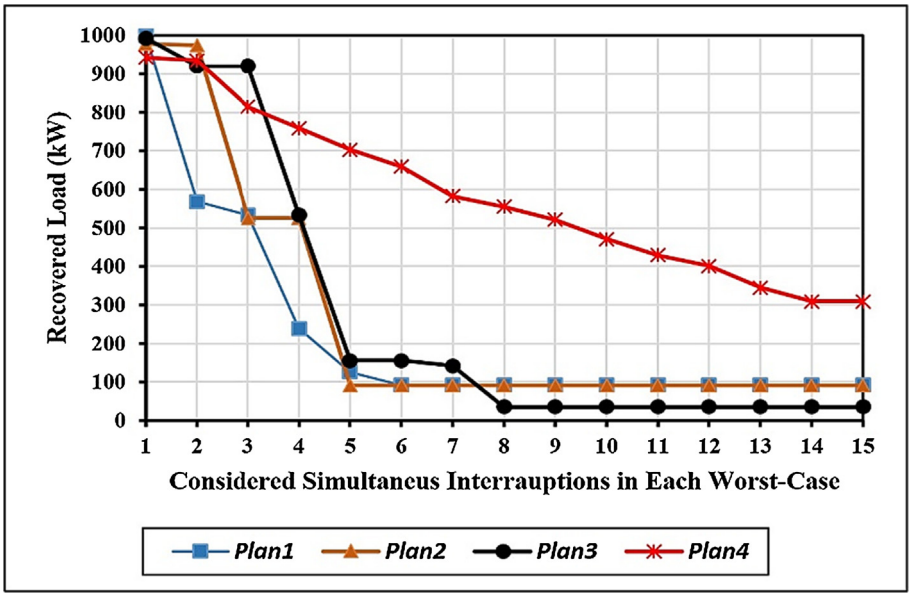

Fig. 8. The performance of each plan in case of worst contingencies.

Table 2
Comparing the SysRes values.

	Plan1	*Plan2*	*Plan3*	*Plan4*
SysRes	0.227245	0.26002	0.292845	0.364121

4. Numerical study

To verify the effectiveness of the proposed algorithms, several case studies were programmed in MATLAB environment. All simulations were executed on a personal computer with Intel Core i7 CPU @ 4 GHz, and 16 GB RAM.

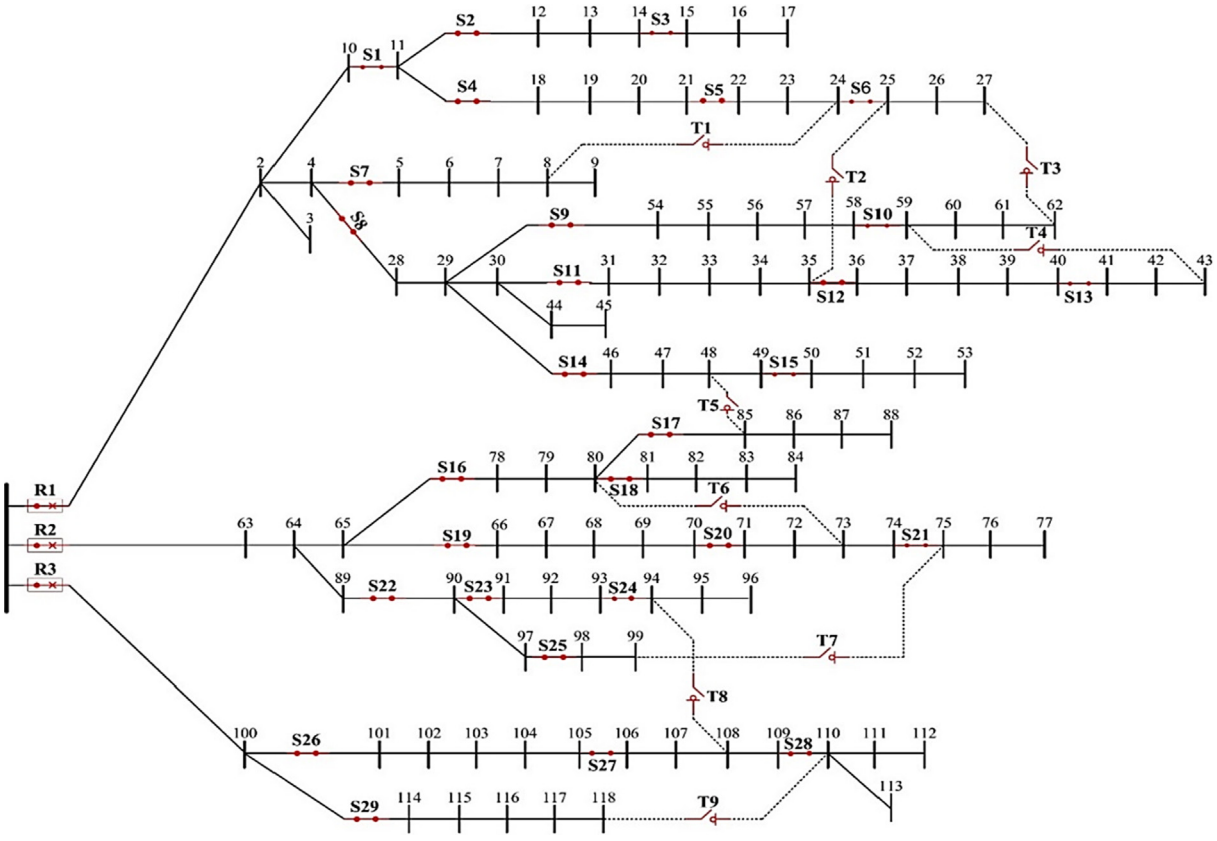

Fig. 9. Single line diagram of the test network II.

Table 3
The capacity and location of DGs.

Unit	Bus	Cap. (kW)	Qmax (kVAr)	Qmin (kVAr)
DG1	17	1000	800	−800
DG2	24	1000	800	−800
DG3	51	1500	1300	−1300
DG4	59	1500	1300	−1300
DG5	67	2000	1800	−1800
DG6	76	1000	800	−800
DG7	107	2500	2200	−2200
DG8	7	100	50	−50
DG9	33	500	350	−350
DG10	88	500	400	−400
DG11	103	500	400	−400
DG12	113	500	400	−400
DG13	92	400	300	−300

Table 4
Data of each section.

Name	Including nodes	Consumption		Generation capacity	
		Active (kW)	Reactive (kVAr)	Active (kW)	Reactive (kVAr)
S1	2, 3, 4, 10	382.569	241.047	0	0
S2	11	146.8	75.995	0	0
S3	12, 13, 14	220.04	159.407	0	0
S4	15, 16, 17	87.67	80.47	1000	800
S5	18, 19, 20, 21	903.774	606.029	0	0
S6	22, 23, 24	346.447	189.422	1000	800
S7	25, 26, 27	167.17	199.46	0	0
S8	5, 6, 7, 8, 9	437.793	256.507	200	150
S9	28, 29, 30, 44, 45	1706.48	1372.721	0	0
S10	54, 55, 56, 57, 58	1422.553	955.532	0	0
S11	59, 60, 61, 62	209.748	159.044	2000	1700
S12	31, 32, 33, 34, 35	1477.06	1087.814	500	350
S13	36, 37, 38, 39, 40	1383.539	1503.739	0	0
S14	41, 42, 43	542.627	380.202	300	200
S15	46, 47, 48, 49	582.048	503.076	0	0
S16	50, 51, 52, 53	261.831	204.444	2000	1700
S17	63, 64, 65, 89	977	839.306	0	0
S18	78, 79, 80	156.13	144.68	0	0
S19	85, 86, 87, 88	1110.69	634.362	400	300
S20	81, 82, 83, 84	260.915	224.714	0	0
S21	66, 67, 68, 69, 70	1006.725	679.323	2000	1800
S22	71, 72, 73, 74	1649.839	961.36	0	0
S23	75, 76, 77	289.489	197.617	1000	800
S24	90, 97	678.33	419.63	0	0
S25	91, 92, 93	972.63	803.98	300	200
S26	94, 95, 96	206.473	173.765	0	0
S27	98, 99	72.113	32.406	0	0
S28	100	100.66	47.572	0	0
S29	101, 102, 103, 104, 105	1633.38	1168.324	500	400
S30	106, 107, 108, 109	1325.303	1026.077	2000	1800
S31	110, 111, 112, 113	1465.99	1328.35	300	200
S32	114, 115, 116, 117, 118	522.904	384.693	0	0

4.1. Test network i

To investigate the advantages of the proposed measure in resiliency analysis of the long-term investment studies, the introduced modularity-based index (SysRes) has been employed for evaluating the generation expansion plans and calculating the effectiveness of the DG placement options from resiliency perspective. As depicted in Fig. 7, a modified 85-bus test system has been considered for simulation. The line parameters and load consumptions data have been provided in [52]. In addition, it is assumed that the system operator or planner, according to Table 1, aims to choose from four different options for allocating 1000 kW generation capacity on this test network to improve the resiliency.

The self-healing capabilities of the mentioned plans for the worst simultaneous k interruptions of the lines have been calculated and depicted in Fig. 8. Obviously, these worst interruptions are different for each plan. For instance, in *Plan3*, simultaneous interruptions of the lines *L1* (between nodes 1 and 2) and *L13* (between nodes 13 and 14) have been the worst double contingencies, but for the *Plan4*, interruptions of the lines *L1* and *L18* (between nodes 18 and 19) have been regarded as the worst double contingencies. In addition, the SysRes levels for these plans have been calculated and tabulated in Table 2.

According to Fig. 8, the *Plan1*, *Plan2*, and *Plan3* have the best performances at the worst single, double, and triple contingencies, respectively. In other words, the mentioned plans have better resiliency based on the worst-case measures compared to the *Plan4*.

It can be inferred from the results that evaluating the aptness of the investment options based on the worst-case principles prepares the system for that particular situation, yet it leads to more fragile configuration against the higher intensities. For example, although, *Plan2* and *Plan3* have the highest recoverability (974.4 kW and 920.1 kW) in case of worst double and triple contingencies, the mentioned schemes are more vulnerable in case of severe conditions ($k > 3$) compared to the modular plan (*Plan4*).

According to the results, the *Plan4*, which has the highest SysRes level, distributes the generation capacities across the network, and correspondingly leads to a more modularized structure compared to the other plans. This yields a more resilient plan in case of multi contingency events. These results emphasize that SysRes index prepares suitable feedbacks to direct the expansion process and provides an appropriate measure for the system planners and decision makers to analyze the investment options wisely from resiliency viewpoint. However, by selecting seven locations for DG installation in *Plan4*, this scheme would be more expensive than the other plans. Evidently, with developing of small-scale distributed generations such as rooftop photovoltaic panels, and reducing the cost of land use requirements, applying *Plan4* will be more economical in future years.

4.2. Test network II

In this section, the proposed model is applied to an 11 kV modified test system [22]. As shown in Fig. 9, the network consists of 3 feeders, 118 buses, 29 sectionalizers, 3 breakers, and 9 tie lines. The total real and reactive power loads are 22.71 MW and 17.04 MVAr, respectively. Detailed information about the load consumptions and line parameters is given in [22]. In this network, there are 13 DGs and among them, seven units (*DG1* to *DG7*) are able to function as a master unit. The location and the capacity of DGs are reported in Table 3.

4.2.1. Case i

In this case, analyzing the system modularity and exploring the host MGs have been taken into consideration. Initially, according to the proposed algorithm, the sectionalized form of the test system is extracted by considering switching capabilities. The required data of each section have been collected in Table 4.

Considering the topological and electrical constraints, the proposed algorithm found 77 structures for MG formation. It can be seen from the results that five sections (*S13*, *S18*, *S20*, *S28*, and *S32*) have not been included in any of the discovered MGs. The MGD, MGPr, and MGE indices for the MGs have been calculated with the results represented in Fig. 10 and Fig. 11.

According to the obtained results, the maximum MGD (lowest independency) belongs to *MG22* (which contains 10 sections and 34 load

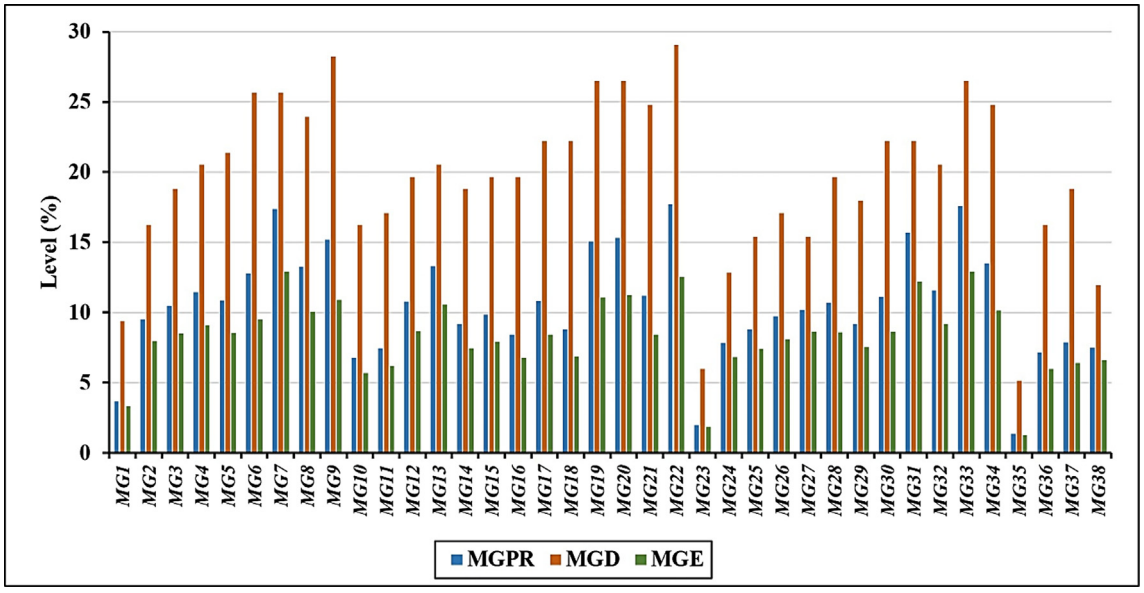

Fig. 10. MGD, MGPr, and MGE indices for *MG1* to *MG38*.

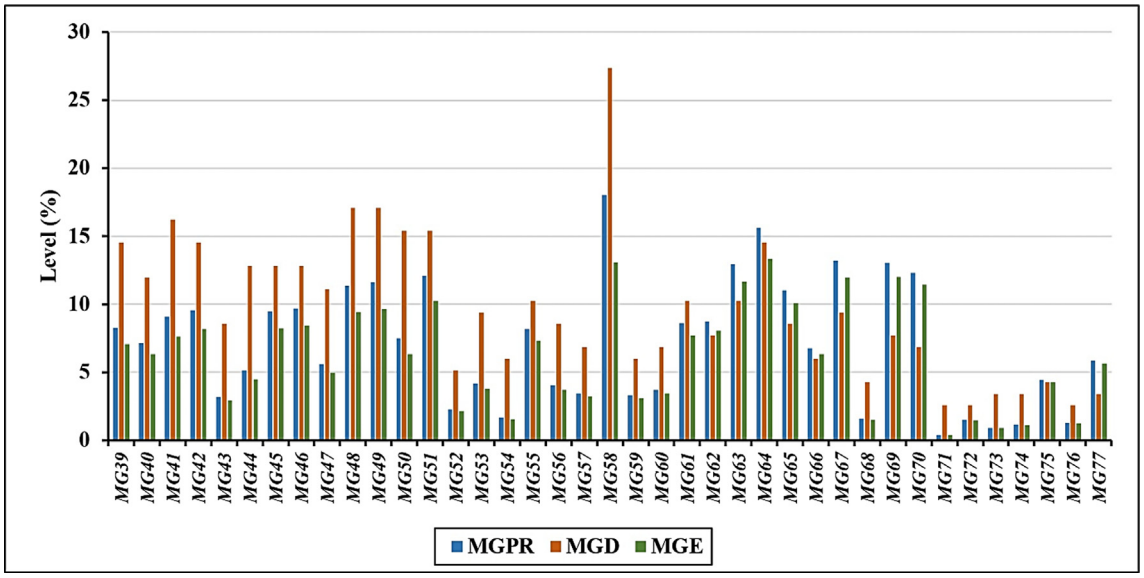

Fig. 11. MGD, MGPr, and MGE indices for *MG39* to *MG77*.

points) with 29.06% value. Further, *MG71*, *MG72*, and *MG76* have the lowest dependency level with 2.56% MGD by including only one section (which is also a master section) and three load points. Finally, the average and standard deviations of the calculated MGD indices have been 14.54% and 7.4%, respectively.

It is also observed that greater profitability for a MG leads to less independency. For example, *MG58* by including 8 sections and 32 load points has the highest MGPr index providing 4.09 MW or 18.03% of the total system consumptions; but this MG is 76th in the independency rank. In this set, *MG71* has the lowest MGPr with 0.386% value. The average and standard deviations of the MGPr indices have been 8.81% and 4.53%. Additionally, *MG64* with 13.34% MGE has the highest efficiency level; by including six sections, 17 load points and providing 3.54 MW this MG is 42nd and 7th in the dependency and profitability ranks, respectively. The average and standard deviations for the calculated MGE indices are 7.26% and 3.42%, respectively.

In addition, the minimum, maximum, and average dependency values for each section are depicted in Fig. 12. For each section, MinHSeD and MaxHSeD values represent the lowest and highest dependency levels of the MGs that contain that section (its host MGs).

It can be inferred from the results that self-provided sections with a master unit, which can be construed as a MG have the lowest MinHSeD value. Further, lower values of AHSeD for a section suggests that this section is generally included in some MGs with a lower number of load points. For example, section *S21* with 7.4% value has the lowest AHSeD. Additionally, since there is only one host MG for sections *S17*, *S29*, *S19*, *S22*, and *S9*, the MinHSeD, MaxHSeD, and AHSeD values are equal for these sections.

The number of the host MGs and the parents for each section are also shown in Fig. 13. It can be inferred that the location of DG units and the switching capability of the network are the main effective factors in determining the host MGs for a section. Based on the results, the sections that include more generation units or have suitable links with others, are included in more MGs. Consequently, these sections are more plausible to be supplied after the events.

The proposed algorithm discovered 34 different arrangements (desired combinations of the independent members of the set EMGs). The efficiency of these combinations is given in Table 5. Member 23 (*A23*)

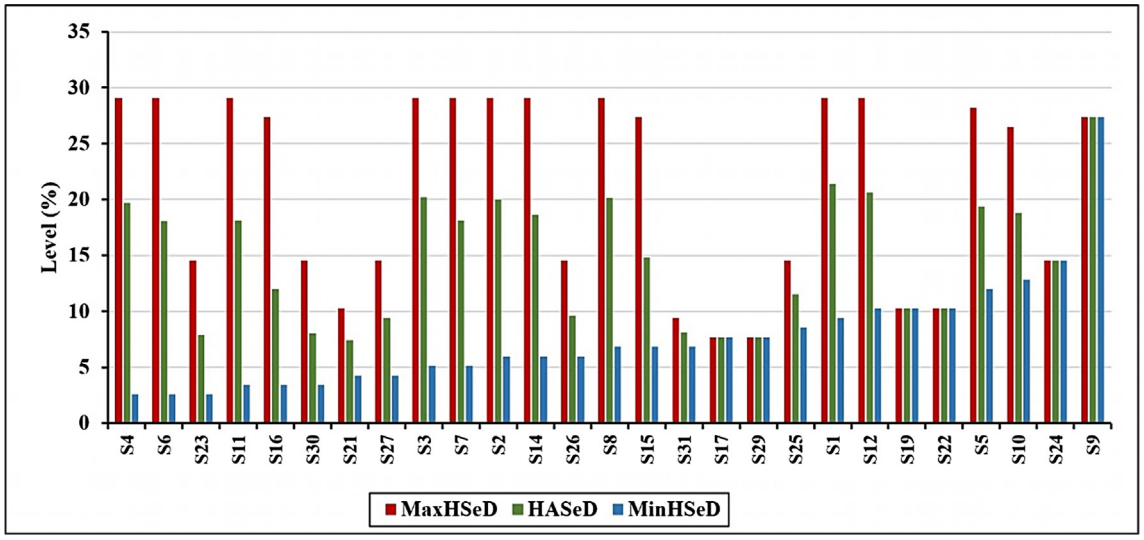

Fig. 12. Section's dependency levels.

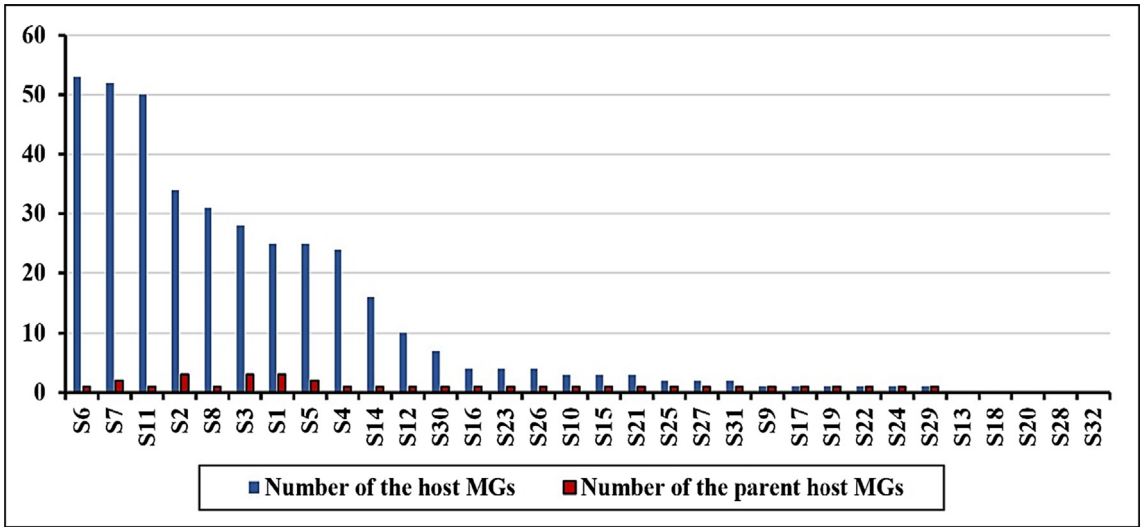

Fig. 13. Number of the host MGs for each section.

Table 5
The efficiency of the extracted combinations.

Name	Efficiency	Name	Efficiency
A1	0.345161	*A18*	0.364466
A2	0.35235	*A19*	0.366559
A3	0.377745	*A20*	0.331636
A4	0.349408	*A21*	0.384295
A5	0.357592	*A22*	0.363863
A6	0.324442	*A23*	0.387788
A7	0.373242	*A24*	0.34841
A8	0.342102	*A25*	0.32786
A9	0.359413	*A26*	0.290417
A10	0.374206	*A27*	0.346602
A11	0.329642	*A28*	0.34727
A12	0.342288	*A29*	0.341516
A13	0.34786	*A30*	0.331989
A14	0.370575	*A31*	0.321675
A15	0.378049	*A32*	0.30696
A16	0.350106	*A33*	0.325038
A17	0.311211	*A34*	0.283364

has the highest efficiency level; therefore, the system resiliency will be 38.78%. This arrangement contains five MGs (*MG1*, *MG40*, *MG61*, *MG62*, and *MG64*) from the set EMGs and supplies 9.46 MW through involving 19 sections. This arrangement is depicted in Fig. 14. Detailed data about the MGs of this arrangement are also reported in Table 6.

Additionally, performing the whole process (path-finding, neighbor analysis, and searching the best arrangement) in this test network takes only 1.91 min, which verifies the computational efficiency of the proposed approach for resiliency analysis.

4.2.2. Case II

In this part, by applying different strategies, the impacts of switching capability and load control (LC) options on the system resiliency are investigated. In the first and third strategies (*ST1* and *ST3*), switching through the tie lines has not been considered. In the third and fourth strategies (*ST3* and *ST4*), applying 20% load curtailments at nine sections (*S5*, *S9*, *S10*, *S12*, *S13*, *S22*, *S29*, *S30*, and *S31*) are permissible. The obtained results are tabulated in Table 7.

Based on the results, by applying the tie lines or LC options, the number of the formable MGs and the modularization level of the system grew by about 8%. Further, by employing these resources, the number of sections not included in any of the host MGs diminished. Since

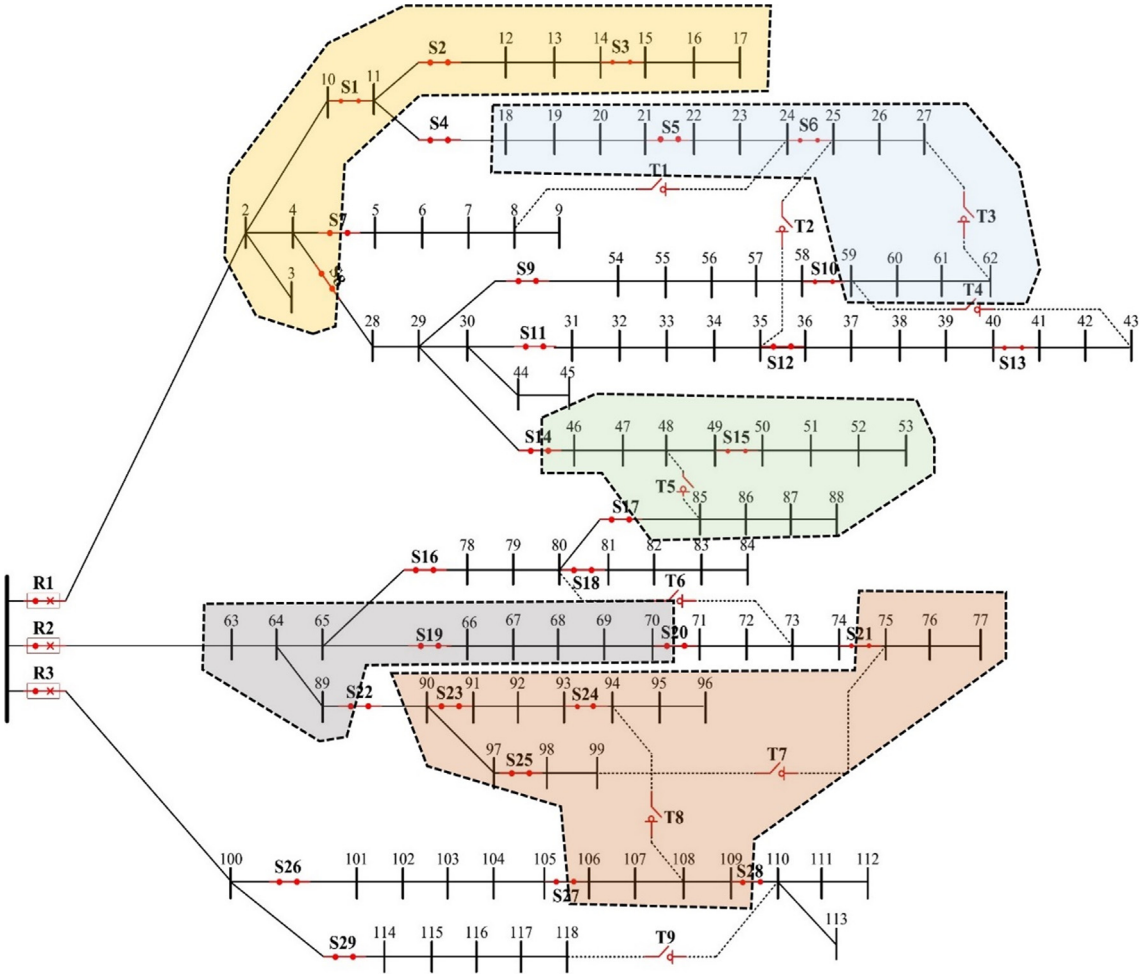

Fig. 14. Servicing areas of the involved MGs in A23.

Table 6
Characteristics of the involved MGs in *A23*.

Name	Involved sections	Number of load points	MGE (%)
MG1	S1, S2, S3, S4	11	3.34
MG40	S5, S6, S7, S11	14	6.31
MG61	S15, S16, S19	12	7.73
MG62	S17, S21	9	8.06
MG64	S23, S24, S25, S26, S27, S30	17	13.34

considering the tie lines increases the number of the paths in the network, therefore, the simulation of the *ST2* and *ST4* takes more time than the *ST1* and *ST3* strategies. It can be inferred that applying these flexibilities in distribution networks enhances modularity and improves the system resiliency as well. Note that the appropriate development of these facilities will be critical to reinforce the distribution network against severe events.

4.2.3. Case III

In this case, the impact of the RESs and load uncertainties on the system resiliency is investigated. For this purpose, six wind turbines with a capacity of 500 kW are connected to the test network II instead of the six units of *DG8* to *DG13*. In this simulation, 10 and 14 different factors are applied for modeling the uncertainties of the load consumptions and output powers of the wind turbines, respectively. In each scenario, corresponding factors are multiplied at the given peak load consumptions in Case I and wind turbine capacities. Required information about these scenarios is given in [53].

Distributions of the SysRes index for various consumption and RES conditions are depicted in Fig. 15 and Fig. 16. According to the results, the maximum, minimum, and expected values of the SysRes index are 0.4256, 0.2736, and 0.3511, respectively. In the best scenario, where the system peak load is 20.65 MW and the total available generation is 13.5 MW (about 65.37% of the load consumptions), SysRes index is enhanced to 0.4256. Similar to the obtained results in the test network I, besides the generation capacities, distribution of these resources is

Table 7
The results for each strategy.

	ST1: No Ties, No LC	*ST2*: with Ties, No LC	*ST3*: No Ties, with LC	*ST4*: with Ties, with LC
Execution time (min)	0.0394	1.911	0.0451	2.27
Number of the host MGs	18	77	22	112
Number of not-involved sections	15	5	12	1
Number of the arrangements	12	34	16	54
System resiliency	33.51%	38.78%	39.84%	41.86%

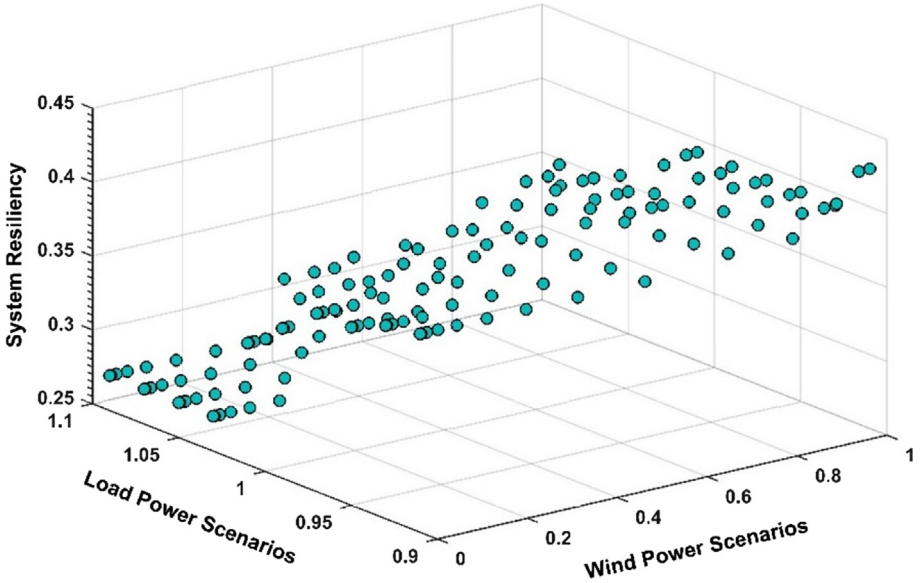

Fig. 15. System resiliency index in considered scenarios.

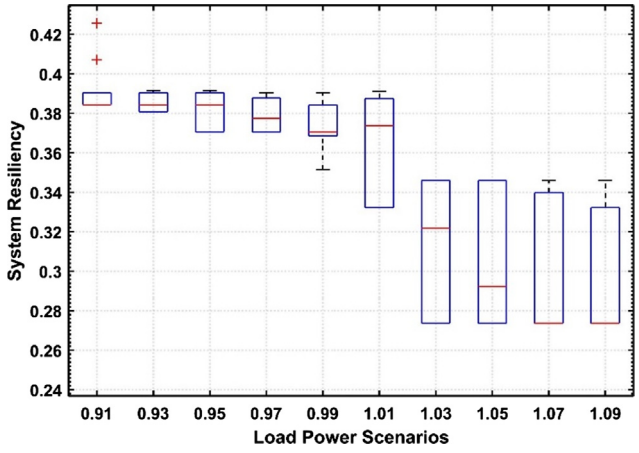

Fig. 16. The impact of the wind generation availability on the system resiliency.

also an important issue in increasing the system resiliency.

Furthermore, the resiliency in the worst condition (highest power consumptions and lowest wind generations) could be 15 percent lower than the best scenario. In addition, unavailability of the RES generations decreases the resiliency about 8% in high load conditions (factors 1.01 to 1.09) and puts the system at serious challenges. These results emphasize that integrating the RES resources to electric distribution systems should be also analyzed from the resiliency perspective.

4.2.4. Case IV

In this part, the proposed method is employed to evaluate the survivability of the sections in case of storm occurrence. Since the extraction of fragility curves and estimation of the failure probabilities are beyond the scope of this paper, the failure probabilities for distribution lines (without switching capability), buses, and interface links have been considered to be 0.06, 0.02, and 0.09 respectively. For the sake of simplicity, the length of each line has been assumed to be 1 km, and DG units are assumed secure against the storm.

In Fig. 17, the survivability of the host MGs has been compared to their dependency levels. It can be seen from the results that MGs with

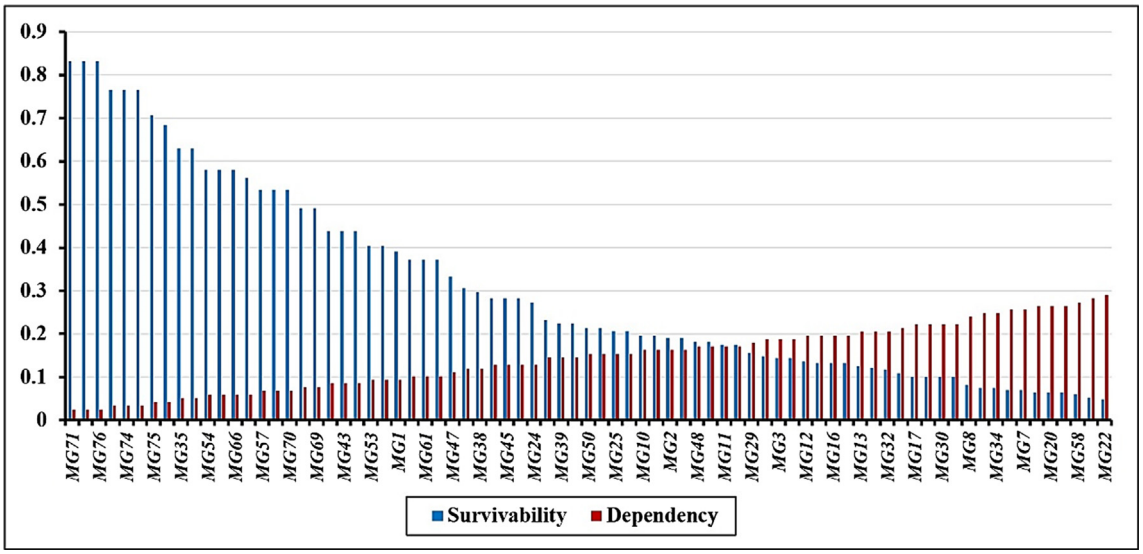

Fig. 17. Survivability and dependency level of the explored MGs.

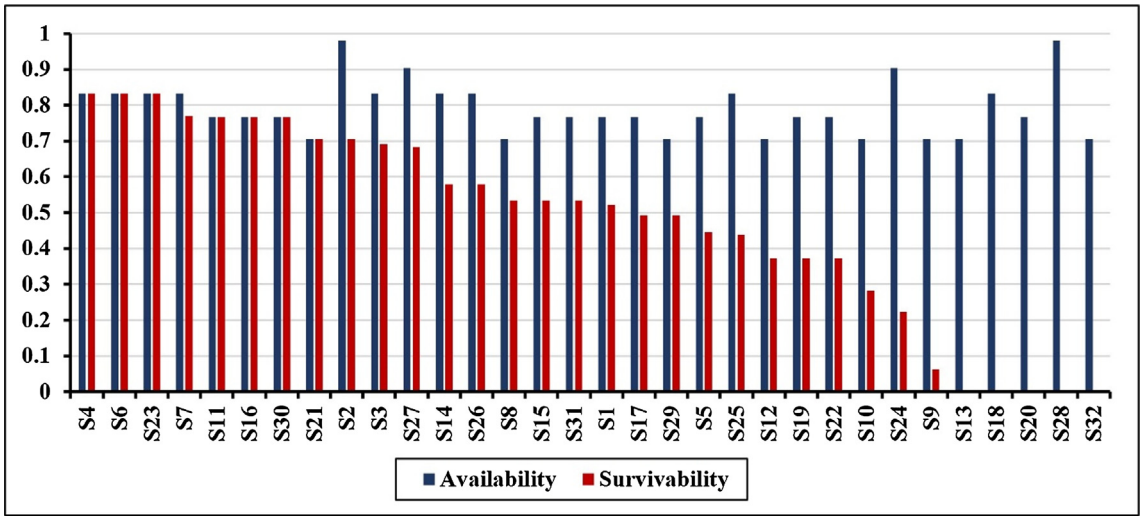

Fig. 18. The performance of sections in case of the storm.

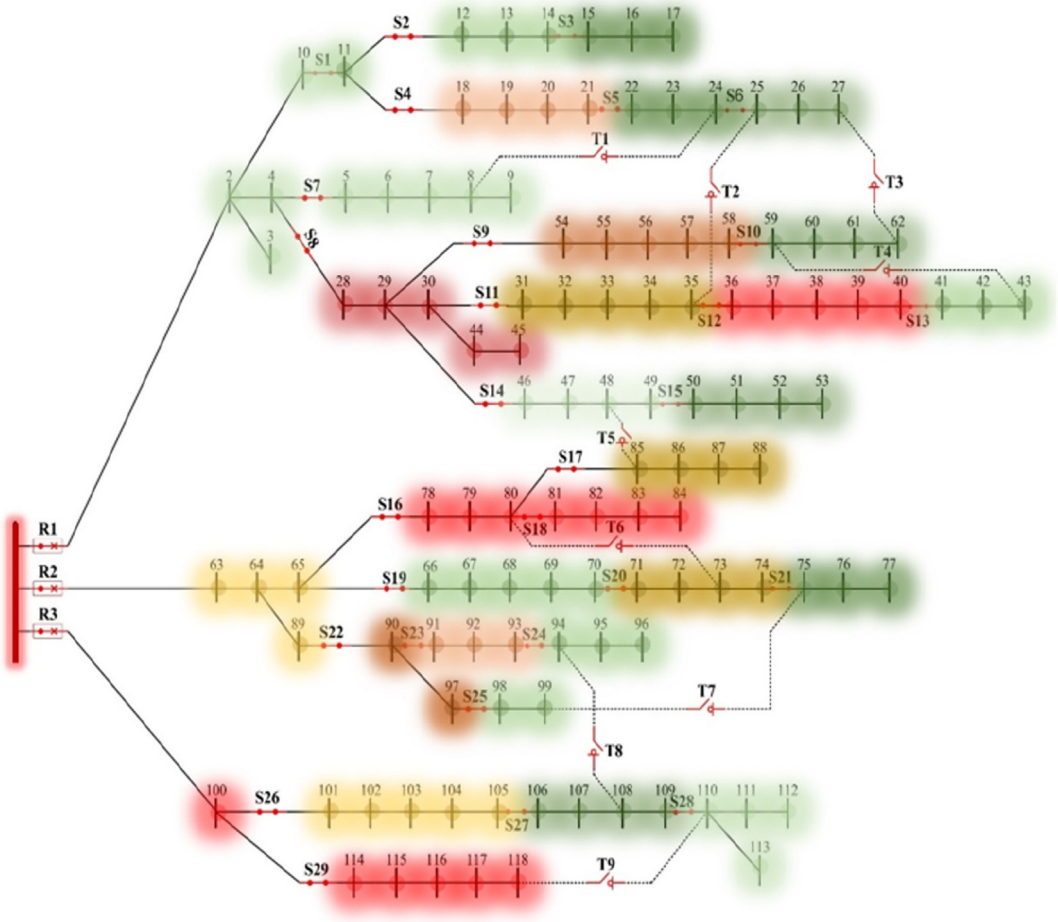

Fig. 19. Sections' survivability status (green: the best, red: the worst). (For interpretation of the references to colour in this figure legend, the reader is referred to the web version of this article.)

fewer load points (higher independency) are more likely to survive after the storm.

Sections' availability and survivability are also illustrated in Fig. 18. Based on the results, master self-provided sections have the highest survivability ranks. It is because of the fact that, if these master sections are available (not damaged) after the storm, certainly they can be restored through their own generations. Further, because of considering secure state for generation units, the survivability and availability values have been equal for the master sections. For the other sections, the resilient operation can be achieved through survival of at least one of their host MGs. Consequently, the survivability levels for the mentioned sections have been lower than their availability values.

In addition, Fig. 18 represents the importance of the section's location and interface links on its survivability. For example, due to the

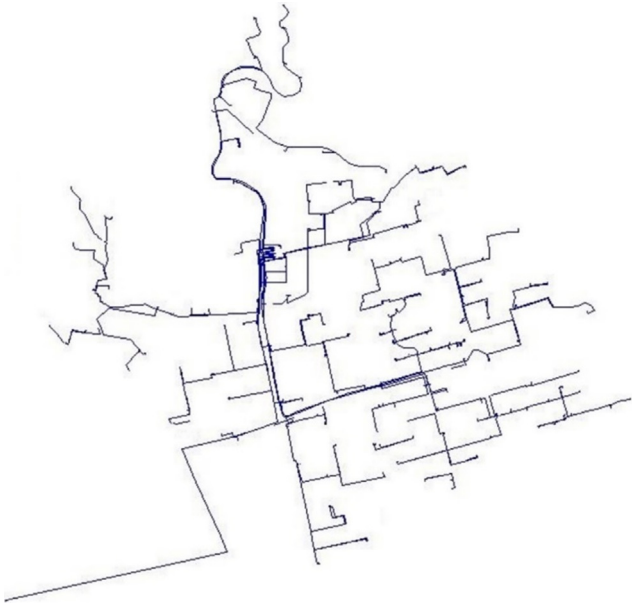

Fig. 20. Test network III.

Table 8
The performance of the main and approximate methods.

DG Capacity (kW)	Main method		Approximate method	
	SysRes	Time (h)	SysRes	Time (min)
500	0.0585	2.3518	0.0585	2.8807
750	0.0742	2.4230	0.0635	2.9126
1000	0.1183	2.8170	0.0887	2.9190
1250	0.1667	3.3624	0.1171	2.9247
1500	0.2508	3.9666	0.2301	2.9372
1750	0.3097	4.5641	0.2893	2.9402
2000	0.4186	6.0633	0.4014	3.0001
2250	0.4873	6.7052	0.4734	3.0452
2500	0.5218	7.5380	0.5066	3.1024

high availability of *S7*, and suitable interfacing with the master sections *S6* and *S11*, this section is one of the most resilient parts of the network.

In addition, performing the analysis takes only 10.61 s. The reason is that, due to the lower number of the parent MGs compared to the hosts (as shown in Fig. 13), applying the idea of the parent MGs in probability calculation process makes an outstanding performance. Survivability status of the sections has also been illustrated in Fig. 19.

4.3. Test network III

In this section, for analyzing the efficiency and applicability of the proposed algorithm, a real 20-kV distribution network (as shown in Fig. 20) is considered for simulation. Servicing areas of this network includes a part of Sa'adat-Abad district in Tehran, Iran. This network contains 14 feeders, 492 buses, 516 lines, 79 sectionalizers, and 25 tie lines. The total active and reactive power loads are 46.739 MW and 15.063 MVAr, respectively. Moreover, it is assumed that 12 DG units with master capabilities are connected to the network. The detailed information about the loads, line parameters, DGs and switch locations are provided in [54].

The resiliency index and execution time of the proposed main and approximate approaches for different DG capacities are calculated and reported in Table 8. According to the results, escalating the generation capacities enhances the MG formation capability for the system, and consequently improves the system modularity. On the other hand, the execution time for exploring the MGs and finding the best arrangement are also increased by escalating the capacity.

Comparing the obtained results represents that the approximate method by sacrificing an acceptable level of the solution accuracy remarkably improves the computation speed and exceedingly reduces the simulation time. Although the large computation burden of the proposed main method (which does not consider the approximate presumptions) limits its application in the online investigation, in our case, which is a simulation study, the execution time is not a constraint.

In addition, according to the results given in Table 8, increasing the generation capacities enhances the resiliency index as well. However, the improvement rate in some case is low. For example, increasing the capacity of DGs from 2250 kW to 2500 kW (3 MW growth in total generations) improves the resiliency only about 3%. This result emphasizes that indiscriminate increasing the capacities is not an efficient and reasonable solution to improve the resiliency. In other words, for facilitating the formation of efficient MGs and achieving desired modularity level, coordinated allocation of switching options and generation capacities would be necessary. This issue will be discussed in our future works.

5. Conclusions

The MG technology brings unprecedented modularity, sustainability, and resiliency to the power grid. In this paper, the modularization level was regarded as an appropriate measure for quantifying the resiliency concept at electric distribution voltage levels. For this purpose, utilizing a path-based method, all self-provided modules were explored. The efficient modules included higher consumption levels, which were less dependent on the system components. In addition, the optimal arrangement of the MGs that provided maximum consumptions with the highest independency was obtained using an efficient DP-based algorithm. The obtained results indicated that the sections including adequate generation capacities or proper interactions with the masters had a better status in survivability rank. The results also highlighted the importance of the switching capabilities, the capacity of DGs, and the load controlling options on the system resiliency level. The simulation results verified that the proposed modularity-based framework is a comprehensive approach, which is capable of analyzing the system behavior from a resiliency perspective at the both short-term and long-term horizons. The system planners and operators can utilize the proposed model and developed indices for diagnosing the system weaknesses against the disasters. In addition, comparing the proposed measure with the previous worst-case indices confirmed that the SysRes index provides the system planner useful information about the resiliency status of the system. It is indeed a more efficient measure particularly for appraising the investment options. Moreover, the simulation results accentuate that the integration of the uncertain renewable resources to the distribution systems may put the system resiliency in serious challenges. Improving the computation efficiency of the proposed algorithm, examining the impact of the other smart grid facilities such as electric vehicles, and developing appropriate models for resiliency enhancement based on the modularity concept are considered as our future works.

Declaration of Competing Interest

The authors declare that they have no known competing financial interests or personal relationships that could have appeared to influence the work reported in this paper.

References

[1] Jufri FH, Widiputra V, Jung J. State-of-the-art review on power grid resilience to extreme weather events: definitions, frameworks, quantitative assessment methodologies, and enhancement strategies. Appl Energy 2019;239:1049–65.
[2] Guerra OJ, Tejada DA, Reklaitis GV. Climate change impacts and adaptation

strategies for a hydro-dominated power system via stochastic optimization. Appl Energy 2019;233:584–98.
[3] Demissie AA, Solomon AA. Power system sensitivity to extreme hydrological conditions as studied using an integrated reservoir and power system dispatch model, the case of Ethiopia. Appl Energy 2016;182:442–63.
[4] Zhou Y, Panteli M, Moreno R, Mancarella P. System-level assessment of reliability and resilience provision from microgrids. Appl Energy 2018;230:374–92.
[5] Nan C, Sansavini G. A quantitative method for assessing resilience of interdependent infrastructures. Reliab Eng Syst Saf 2017;157:35–53.
[6] Hosseini S, Barker K, Ramirez-Marquez JE. A review of definitions and measures of system resilience. Reliab Eng Syst Saf 2016;145:47–61.
[7] Hussain A, Bui VH, Kim HM. Microgrids as a resilience resource and strategies used by microgrids for enhancing resilience. Appl Energy 2019;240:56–72.
[8] Kahnamouei AS, Bolandi TG, Haghifam MR. The conceptual framework of resilience and its measurement approaches in electrical power systems. IET International conference on resilience of transmission and distribution networks (RTDN). Birmingham, UK. 2017.
[9] Li Zhiyi, Shahidehpour Mohammad, Aminifar Farrokh, Alabdulwahab Ahmed, Al-Turki Yusuf. Networked microgrids for enhancing the power system resilience. In: Proceedings of the IEEE; 2017.
[10] Jiménez-Estévez G, Navarro-Espinosa A, Palma-Behnke R, Lanuzza L, Velázquez N. Achieving resilience at distribution level: learning from isolated community microgrids. IEEE Power Energ Mag 2017;15(3):64–73.
[11] Gholami A, Aminifar F, Shahidehpour M. Front lines against the darkness: Enhancing the resilience of the electricity grid through microgrid facilities. IEEE Electri Mag 2016;4(1):18–24.
[12] Lai K, Illindala M, Subramaniam K. A tri-level optimization model to mitigate coordinated attacks on electric power systems in a cyber-physical environment. Appl Energy 2019;235:204–18.
[13] Ton DT, Wang WP. A more resilient grid: The US department of energy joins with stakeholders in an R&D plan. IEEE Power Energ Mag 2015;13(3):26–34.
[14] Wang Y, Chen C, Wang J, Baldick R. Research on resilience of power systems under natural disasters—a review. IEEE Trans Power Syst 2016;31(2):1604–13.
[15] Moslehi S, Reddy TA. A new quantitative life cycle sustainability assessment framework: application to integrated energy systems. Appl Energy 2019;239:482–93.
[16] Zhang B, Dehghanian P, Kezunovic M. Optimal allocation of PV generation and battery storage for enhanced resilience. IEEE Trans Smart Grid 2017. https://doi.org/10.1109/TSG.2017.2747136.
[17] Cai B, Xie M, Liu Y, Liu Y, Feng Q. Availability-based engineering resilience metric and its corresponding evaluation methodology. Reliab Eng Syst Saf 2018;172:216–24.
[18] Moslehi S, Reddy TA. Sustainability of integrated energy systems: a performance-based resilience assessment methodology. Appl Energy 2018;228:487–98.
[19] Chanda S, Srivastava AK. Defining and enabling resiliency of electric distribution systems with multiple microgrids. IEEE Trans Smart Grid 2016;7(6):2859–68.
[20] Bajpai P, Chanda S, Srivastava AK. A novel metric to quantify and enable resilient distribution system using graph theory and Choquet integral. IEEE Trans Smart Grid 2018;9(4):2918–29.
[21] Zare-Bahramabadi M, Abbaspour A, Fotuhi-Firuzabad M, Moeini-Aghtaie M. Resilience-based framework for switch placement problem in power distribution systems. IET Gener Transm Distrib 2017;12(5):1223–30.
[22] Ma S, Su L, Wang Z, Qiu F, Guo G. Resilience enhancement of distribution grids against extreme weather events. IEEE Trans Power Syst 2018;33(5):4842–53.
[23] Amirioun MH, Aminifar F, Lesani H. Resilience-oriented proactive management of microgrids against windstorms. IEEE Trans Power Syst 2018;33(4):4275–84.
[24] Mousavizadeh S, Haghifam MR, Shariatkhah MH. A linear two-stage method for resiliency analysis in distribution systems considering renewable energy and demand response resources. Appl Energy 2018;211:443–60.
[25] Rocchetta R, Zio E, Patelli E. A power-flow emulator approach for resilience assessment of repairable power grids subject to weather-induced failures and data deficiency. Appl Energy 2018;210:339–50.
[26] Fang Y, Sansavini G. Optimizing power system investments and resilience against attacks. Reliab Eng Syst Saf 2017;159:161–73.
[27] Rahimi K, Davoudi M. Electric vehicles for improving resilience of distribution systems. Sustain Cities Society 2018;36:246–56.
[28] Dessavre DG, Ramirez-Marquez JE, Barker K. Multidimensional approach to complex system resilience analysis. Reliab Eng Syst Saf 2016;149:34–43.
[29] Yuan W, Wang J, Qiu F, Chen C, Kang C, Zeng B. Robust optimization-based resilient distribution network planning against natural disasters. IEEE Trans Smart Grid 2016;7(6):2817–26.
[30] Chanda S, Srivastava AK, Mohanpurkar MU, Hovsapian R. Quantifying power distribution system resiliency using code-based metric. IEEE Trans Indust Apps 2018;54(4):3676–86.
[31] Trakas DN, Hatziargyriou ND. Optimal distribution system operation for enhancing resilience against wildfires. IEEE Trans Power Syst 2018;33(2):2260–71.
[32] He C, Dai C, Wu L, Liu T. Robust network hardening strategy for enhancing resilience of integrated electricity and natural gas distribution systems against natural disasters. IEEE Trans Power Syst 2018;33(5):5787–98.
[33] Ma S, Chen B, Wang Z. Resilience enhancement strategy for distribution systems under extreme weather events. IEEE Trans Smart Grid 2018;9(2):1442–51.
[34] Gentile PD. Theory of modularity, a hypothesis. Proce Comput Sci 2013;20:203–9.
[35] Jackson S. Principles for resilient design – a guide for understanding and implementation. In: Linkov I, editor. IRGC resource guide on resilience. University of Lausanne, Switzerland: Int Risk Governance Counc (IRGC); 2016.
[36] Rus K, Kilar V, Koren D. Resilience assessment of complex urban systems to natural disasters: a new literature review. IntJ Disaster Risk Reduc 2018;May:26.
[37] Zhang B, Huang G, Zheng Z, Ren J, Hu C. Approach to mine the modularity of software network based on the most vital nodes. IEEE Access 2018:29.
[38] Mutingi M, Dube P, Mbohwa C. A modular product design approach for sustainable manufacturing in a fuzzy environment. Procedia Manuf 2017;8:471–8.
[39] Wang S, Zhang J, Zhao M, Min X. Vulnerability analysis and critical areas identification of the power systems under terrorist attacks. Phys A 2017;473:156–65.
[40] Wang S, Zhang J, Duan N. Multiple perspective vulnerability analysis of the power network. Phys A 2018;492:1581–90.
[41] Wei D, Zhang X, Mahadevan S. Measuring the vulnerability of community structure in complex networks. Reliab Eng Syst Saf 2018;174:41–52.
[42] Zhang CW, Zhang T, Chen N, Jin T. Reliability modeling and analysis for a novel design of modular converter system of wind turbines. Reliab Eng Syst Saf 2013;111:86–94.
[43] Andresen M, Costa LF, Buticchi G, Liserre M. Smart transformer reliability and efficiency through modularity. Power electron motion control conference (IPEMC-ECCE Asia). 2016. p. 3241–8.
[44] Zhou R, Hansen EA. Breadth-first heuristic search. Artif Intell 2006;170(4–5):385–408.
[45] Hameed F, Al Hosani M, Zeineldin HHA. modified backward/forward sweep load flow method for islanded radial microgrids. IEEE Trans Smart Grid 2017;10(1):910–8.
[46] Li H, Mao W, Zhang A, Li C. An improved distribution network reconfiguration method based on minimum spanning tree algorithm and heuristic rules. Int J Electr Power Energy Syst 2016;82:466–73.
[47] Ahmadi H, Martí JR. Mathematical representation of radiality constraint in distribution system reconfiguration problem. Int J Electr Power Energy Syst 2015;64:293–9.
[48] Shariatkhah MH, Haghifam MR, Salehi J, Moser A. Duration based reconfiguration of electric distribution networks using dynamic programming and harmony search algorithm. Int J Electr Power Energy Syst 2012;41(1):1–10.
[49] Panteli M, Mancarella P. Modeling and evaluating the resilience of critical electrical power infrastructure to extreme weather events. IEEE Sys J 2017;11(3):1733–42.
[50] Navarro-Espinosa A, Moreno R, Lagos T, Ordoñez F, Sacaan R, Espinoza S, et al. Improving distribution network resilience against earthquakes. IET international conference on resilience of transmission and distribution networks (RTDN). Birmingham, UK. 2017.
[51] Panteli M, Pickering C, Wilkinson S, Dawson R, Mancarella P. Power system resilience to extreme weather: fragility modeling, probabilistic impact assessment, and adaptation measures. IEEE Trans Power Syst 2016;32(5):3747–57.
[52] Das D, Kothari DP, Kalam A. Simple and efficient method for load flow solution of radial distribution networks. Int J Electr Power Energy Syst 1995;17(5):335–46.
[53] https://www.dropbox.com/s/isfxzav21zmg0kr/Uncertainties.xlsx?dl=0/ [accessed 13 October 2018].
[54] https://www.dropbox.com/s/dz5a382qnl9g385/SaadatAbad-RESS.xlsx?dl=0/ [accessed 13 October 2018].